Hindawi Publishing Corporation
Advances in Materials Science and Engineering
Volume 2014, Article ID 198620, 8 pages
http://dx.doi.org/10.1155/2014/198620

Research Article

A Novel Approach to Measure the Hydraulic Capacitance of a Microfluidic Membrane Pump

Chun-Hui Wu, Chia-Wei Chen, Long-Sheng Kuo, and Ping-Hei Chen

Department of Mechanical Engineering, National Taiwan University, No. 1, Roosevelt Road, Section 4, Taipei 10617, Taiwan

Correspondence should be addressed to Ping-Hei Chen; phchen@ntu.edu.tw

Received 15 January 2014; Revised 6 May 2014; Accepted 15 May 2014; Published 1 June 2014

Academic Editor: Jun Liu

A novel approach was proposed to measure the hydraulic capacitance of a microfluidic membrane pump. Membrane deflection equations were modified from various studies to propose six theoretical equations to estimate the hydraulic capacitance of a microfluidic membrane pump. Thus, measuring the center deflection of the membrane allows the corresponding pressure and hydraulic capacitance of the pump to be determined. This study also investigated how membrane thickness affected the Young's modulus of a polydimethylsiloxane (PDMS) membrane. Based on the experimental results, a linear correlation was proposed to estimate the hydraulic capacitance. The measured hydraulic capacitance data and the proposed equations in the linear and nonlinear regions qualitatively exhibited good agreement.

1. Introduction

A membrane pump is a key component for transporting fluids in microfluidic systems, and such pumps can be categorized based on their actuating strategies: electrostatic [1], piezoelectric [2, 3], electromagnetic [3, 4], and hand-powered [5–8]. Membranes typically comprise parylene [1], silicon [2], polyester [3], silicone [6], or polydimethylsiloxane (PDMS) [5, 7, 8]. PDMS has been a focus in microfluidic devices because it can be rapidly fabricated and exhibits biocompatibility, and its transparency facilitates optical analysis. Most pumps actuated by electric power are fabricated using complicated processes because of complex electrode configurations and the use of microelectromechanical systems or micromachining technologies. Alternative fabrication methods have been proposed to address these drawbacks [5, 8].

Electrohydraulic analogy theory (EAT) [9–11] is a theory used to establish a relation between electrical and hydraulic circuits, elucidating hydraulic circuits. The core idea of EAT is that hydraulic circuits can be analogous to electrical circuits in case the relations are both linear. Similar to the Hagen-Poiseuille law in hydrodynamics, Ohm's law states that, in electrical circuits, the pressure drop and volumetric flow rates are analogous to the electric potential and current, respectively. The hydraulic resistance is analogous to the electrical resistance. It is imperative that flow be conserved at all nodes of the fluid circuit network and the pressure should be totally consumed around any closed loop in fluid circuit. The advantage of EAT is that it can estimate the required pressure when the flow rate is given in a hydraulic circuit. Similar to thermal resistance, an algebraic expression can be used for qualitative description or quantitative estimation. EAT is suitable for use with laminar, incompressible flows; thus, it is suitable for use in microfluidic systems. EAT also establishes a relation between macrofluidic and microfluidic dynamics that can serve as a reference.

Viscosity, inertia, and compressibility effects cause hydraulic resistance, hydraulic inductance, and hydraulic capacitance in fluidic circuits. Although various approaches have been proposed to measure the hydraulic resistance [9, 10], references about the hydraulic capacitance are limited [12, 13]. A membrane pump typically exhibits high hydraulic capacitance because its structure allows large volume changes from the pumping chamber. Thus, a novel approach to measure the hydraulic capacitance of a PDMS-made microfluidic membrane pump is proposed in this study.

2. Theory and Measurement Method

2.1. Electrohydraulic Analogy Theory. Assuming that a steady Hagen-Poiseuille flow passes through a straight circular

channel at a constant flow rate, pressure drops between the inlet and the outlet of the channel because of the viscosity effect. The linear relation between pressure drops and volumetric flow rates in a channel is the Hagen-Poiseuille law, which is typically applicable, even when the flow passes through complex networks in conjunction with the conservation of mass. The simplified linear relation between pressure drops and volumetric flow rates is expressed as follows:

$$\Delta P = \frac{128\mu L}{\pi D_i^4} Q, \tag{1}$$

where ΔP is the pressure drop, μ is the fluid viscosity, L is the channel length, D_i is the inner diameter of the channel, and Q is the volumetric flow rate. Thus, the hydraulic resistance of a uniform circular cross-sectional channel can be defined as follows because of the viscosity effect:

$$R_h = \frac{128\mu L}{\pi D_i^4}. \tag{2}$$

Equation (2) can be extended by using the hydraulic diameter if the cross-section of the pipe is not circular. For a rectangular cross-sectional channel, this substitution yields an approximately 20% overestimation in hydraulic resistance [9].

Furthermore, additional effects must be considered in fluid dynamics. When the inlet flow is an intermittent flow and it fluctuates with respect to frequency, the input pressure is time dependent; thus, the inertia and compressibility effects (also called the hydraulic inductance and hydraulic capacitance) should be addressed. The inductor and capacitor in the electric circuit are available when AC is applied instead of DC; therefore, the hydraulic inductance and hydraulic capacitance can be analogous to the inductor and capacitor in an electric circuit. Regarding channels, a transporting fluid must overcome the pressure drops caused by the viscosity effect, and the rest of pressure drops are subsequently consumed by the inertia of transporting a fluid, providing fluid to accelerate or decelerate movement in a hydraulic circuit. Based on Newton's second law, the force per unit area required to accelerate a fluid slug that exhibits the length l and cross-sectional area S is defined as follows:

$$\Delta P = \frac{\rho l}{S} \frac{dQ}{dt}, \tag{3}$$

where ρ is the fluid density. In the same analogous manner, the hydraulic inductance of a uniform cross-sectional channel affected by the inertia effect can be defined as follows:

$$L_h = \frac{\rho l}{S}. \tag{4}$$

After the fluid density, length, and cross-sectional area are determined, the hydraulic inductance of the channel can be estimated. However, masses of fluid in microfluidic systems are typically small; thus, the influence of the inertia effect is extremely small compared with that of the viscosity effect. Generally, the inertia effect must be considered when the input frequency is higher than 30 Hz [11, 12].

Hydraulic capacitance occurs when the viscosity and inertia effects occur simultaneously and are affected by the same pressure drops between the inlet and the outlet. The hydraulic capacitance is defined as the volume change per unit pressure of variation as follows:

$$Q = \frac{dV}{dP} \frac{dP}{dt} = C_h \frac{dP}{dt}, \tag{5}$$

where V is the change in volume due to the applied pressure, P is the applied pressure, and t is the time.

Hydraulic capacitance should not be ignored when (i) the structure of the system is flexible; (ii) bubbles exist inside the system; or (iii) the fluid inside the system is compressible. When using a flexible material, such as PDMS, flexibility affects fluid transportation. Fluid-structure interactions require that the hydraulic capacitance be considered. In addition, bubbles are more compressible than fluids; thus, fluids occupy the vacancies caused when bubbles shrink because of pressure. Furthermore, fluid compressibility affects the hydraulic capacitance. In this study, bubbles were carefully removed when conducting experiments. Deionized water was chosen as the working fluid because of its incompressibility. In other words, the structure affected hydraulic capacitance is the only factor that must be considered.

3. Pressure-Deflection Relation of the Membrane

Based on the definition of the hydraulic capacitance, the pressure change is the primary problem when measuring the hydraulic capacitance of the microfluidic membrane pump. The pressure-deflection relation of the membrane provides an alternative solution, allowing membrane deflection to be measured without measuring the pressure applied to that membrane. The microfluidic modular pump membrane elastically deforms, discharging fluid from the pumping chamber when external force is applied. Figure 1 shows a side view of the modular pump membrane (a) before and (b) while the external force is applied. Figure 1(c) shows the scheme of the microfluidic modular membrane pump. Because the shape of the pumping chamber is hemispherical, the volume change caused by membrane deflection can be defined using the following spherical cap equation:

$$V_{\text{deflection}} = \frac{\pi\delta}{6}\left(3R^2 + \delta^2\right), \tag{6}$$

where $V_{\text{deflection}}$ is the volume change caused by membrane deflection, δ is the center deflection and also the maximal deflection of a circular membrane when uniform external force is applied, and R is the radius of the pumping chamber. The pressure-deflection relation for circular and boundary-bonded membrane was modeled in the literatures [6, 12, 14–16]. Poisson's ratio for PDMS is 0.5 [14]; thus, the

pressure-deflection relation of a membrane for the center point can be expressed as follows:

$$\delta_{\text{linear}} = \frac{9R^4}{64Eh^3}p, \tag{7}$$

$$\delta_{\text{nonlinear}} = h\left(\frac{3R^4}{16Eh^4}\right)^{1/3} p^{1/3}, \tag{8}$$

where E is the elastic modulus of the membrane, h is the membrane thickness, and p is the applied pressure. Linear or nonlinear deflection is distinguished by $\delta < h$ or $\delta > h$, respectively [14]. Equations (7) and (8) hold when $R > 8h$, which is a condition satisfied by the modular pump designed in this study. From (6), $V_{\text{deflection}}$ is function of R and δ; δ is a function of R, E, h, and p. Thus, the total derivative of $V_{\text{deflection}}$ regarding p can be expressed as follows:

$$\begin{aligned}\frac{dV_{\text{deflection}}}{dp} = {} & \frac{\partial V_{\text{deflection}}}{\partial p} + \frac{\partial V_{\text{deflection}}}{\partial R}\frac{dR}{dp} \\ & + \frac{\partial V_{\text{deflection}}}{\partial h}\frac{dh}{dp} + \frac{\partial V_{\text{deflection}}}{\partial E}\frac{dE}{dp},\end{aligned} \tag{9}$$

where the hydraulic capacitance is defined on the left side. The second term on the right side, the radius term, vanishes if R is a constant. The third and fourth terms on the right side show that thickness and elasticity variations of the membrane affect estimating the hydraulic capacitance. Because there are no theoretical relations for dE/dp and dh/dp, (9) is simplified by neglecting the elasticity term and assuming linear dependence between h and p. Thus, it can be approximated as follows:

$$\frac{dV_{\text{deflection}}}{dp} = \frac{\partial V_{\text{deflection}}}{\partial p} + \frac{\partial V_{\text{deflection}}}{\partial h}\left(\frac{h_i - h_o}{p_i - p_o}\right), \tag{10}$$

where h_i is the membrane thickness at any instant with applied pressure, h_o is the original thickness lacking applied pressure, p_i is applied pressure at any instant, and p_o is the original applied pressure, which is zero in this case. The membrane becomes thinner when the applied pressure increases because the membrane boundary is bonded. Considering variations in thickness, the relation between thickness and center deflection is derived by determining the volume conservation of the membrane inside the pumping chamber; this is expressed as follows:

$$h_i = \frac{R^2 h_o}{R^2 + \delta^2}. \tag{11}$$

This equation holds, assuming that h_i and h_o are constant throughout the pumping chamber. When (11) is substituted into (10), the hydraulic capacitance considering the thickness term can be approximated as follows:

$$\begin{aligned}C_{\text{linear}} = {} & \pm\left(\frac{\partial V_{\text{deflection}}}{\partial p} + \frac{\partial V_{\text{deflection}}}{\partial h}\frac{\Delta h}{\Delta p}\right)_{\text{linear}} \\ = {} & \pm\frac{9\pi R^4}{128Eh^3}\left(R^2 + 4\delta^2\right),\end{aligned} \tag{12}$$

$$\begin{aligned}C_{\text{nonlinear}} = {} & \pm\left(\frac{\partial V_{\text{deflection}}}{\partial p} + \frac{\partial V_{\text{deflection}}}{\partial h}\frac{\Delta h}{\Delta p}\right)_{\text{nonlinear}} \\ = {} & \pm\frac{\pi R^4}{32Eh}\left(\frac{R^2}{\delta^2} + \frac{R^2}{R^2 + \delta^2}\right),\end{aligned} \tag{13}$$

where the plus and minus symbols in (12) and (13) refer to the charge and discharge behaviors of the membrane pump, respectively. Furthermore, if the thickness effect is neglected which means only the pressure term is considered, the hydraulic capacitance can be approximated by substituting (7) and (8) into (6) as follows:

$$\begin{aligned}C_{\text{linear}} &= \pm\frac{\partial V_{\text{deflection}}}{\partial p}_{\text{linear}} = \pm\frac{9\pi R^4}{128Eh^3}\left(R^2 + \delta^2\right), \\ C_{\text{nonlinear}} &= \pm\frac{\partial V_{\text{deflection}}}{\partial p}_{\text{nonlinear}} = \pm\frac{\pi R^4}{32Eh}\left(\frac{R^2}{\delta^2} + 1\right).\end{aligned} \tag{14}$$

The total derivative of $V_{\text{deflection}}$ regarding p can be further simplified by assuming linear dependence between $V_{\text{deflection}}$ and p; that is, $\Delta V_{\text{deflection}}/\Delta p = (V_{\text{deflection}} - V_o)/(p - p_o)$, where V_o and p_o are the original volume and pressure change and are set to zero in their original states. Given this assumption, simplified equations for hydraulic capacitance in linear and nonlinear regions can be expressed as follows:

$$\begin{aligned}C_{\text{linear}} &= \pm\frac{\Delta V_{\text{deflection}}}{\Delta p}_{\text{linear}} = \pm\frac{9\pi R^4}{128Eh^3}\left(R^2 + \frac{\delta^2}{3}\right), \\ C_{\text{nonlinear}} &= \pm\frac{\Delta V_{\text{deflection}}}{\Delta p}_{\text{nonlinear}} = \pm\frac{\pi R^4}{32Eh}\left(\frac{3R^2}{\delta^2} + 1\right).\end{aligned} \tag{15}$$

Curves for theoretically estimating the hydraulic capacitance are derived by substituting all parameters into (12)–(15), depending on the linear or nonlinear region in which δ islocated. However, theelastic modulus of a PDMS membrane is not constant at all membrane thicknesses because, in addition to initial membrane thickness [17], it is influenced by curing conditions and fabrication procedures. Where the curing conditions refer to the heating time, heating temperature, cooling time, and cooling temperature, fabrication procedures refer to the stirring and vacuumed time. Thus, to thoroughly investigate hydraulic capacitance, the elastic modulus of a PDMS membrane must be known. In this study, tensile tests were conducted to determine the elastic modulus of a PDMS membrane.

4. Experimental Apparatus and Measurement Method

4.1. Fabricating the Modular Pump and Membrane. The dimensions of the microfluidic modular membrane pump were 20 mm × 20 mm × 10 mm and the diameter of the channel was 0.5 mm. Figure 1(c) shows the scheme of the pump. A mixture of PDMS prepolymer and curing agent (10 : 1 w/w, Sylgard 184 silicone elastomer, Dow Corning) was poured into aluminum molds to fabricate a PDMS-made modular pump and membrane. The aluminum molds

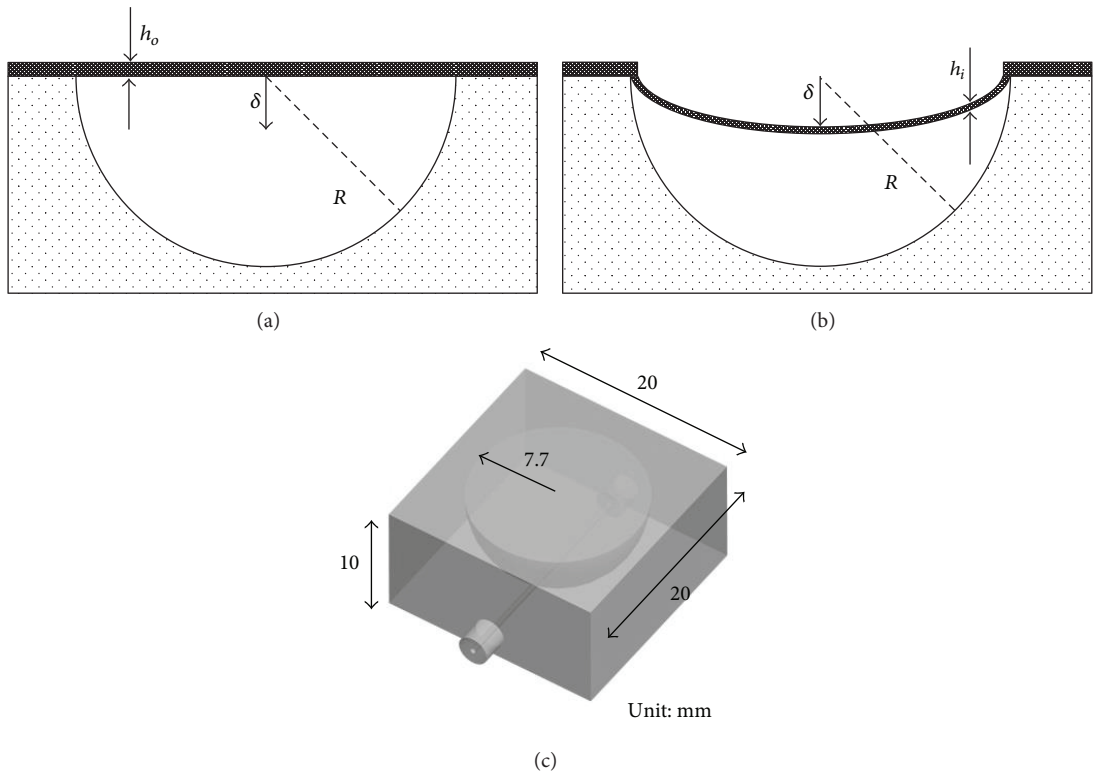

Figure 1: Side view of the modular membrane pump (a) before and (b) while external force is applied. (c) Scheme of the modular pump.

were fabricated using computer numerical control milling. Before pouring, the mixture was stirred for 20 min to ensure that the PDMS prepolymer was thoroughly mixed with the curing agent. The mixture was subsequently vacuumed for 30 min to remove the bubbles generated during stirring. The PDMS-filled mold was placed in an oven at 100°C for 1 h and cooled at room temperature for 1 day. The mold was then removed, the PDMS membrane was glued on top of the modular pump by using the same mixture, and the heating procedure was repeated. This fabrication method yielded PDMS modular pumps for measuring hydraulic capacitance and PDMS membranes for conducting tensile tests.

4.2. Measuring the Elastic Modulus of the PDMS Membrane. The elastic modulus of the PDMS membrane was measured by conducting tensile testing and using the slope of the initial linear region in a true strain-stress curve. A testing specimen was prepared by following the ASTM D 412 test standard for vulcanized rubber and thermoplastic elastomers. The loading speed is 3 mm/s for all tests. Four thicknesses of PDMS membranes (0.3, 0.5, 0.7, and 1.0 mm) were used and 10 test specimens were prepared for each thickness. An MTS Criterion Model 42 tensile test machine was used to conduct the tensile tests; the apparatus accuracy for displacement is 0.1 μm. The specimens were mounted onto a pneumatic grip and held firmly. The speed celerity is 3 mm/s for all tests. The reason why the true stress and true strain are used instead of using engineering stress and engineering strain is because (i) PDMS is an elastomer which can withstand large amounts of strain before fracture; (ii) true stress considers the change in area which matches to the real situation during tensile tests. True strain and true stress were used in the analysis rather than engineering strain and engineering stress. The engineering stress of the PDMS specimen is calculated by using the equation $\sigma_E = F/A_o$, where F is the applied tensile force and A_o is the original cross-section area of the specimen. The engineering strain of the specimen is calculated by using the equation $\varepsilon_o = \Delta L/L_o$, where ΔL is the elongation of the specimen and L_o is the original gauge length of the specimen. The true strain and true stress of the specimen are calculated by using the equation $\varepsilon_T = \ln(1+\varepsilon_E)$, $\sigma_T = \sigma_E(1+\varepsilon_E)$. Young's modulus was calculated based on the initial linear regions of the true stress-strain curves and determined using Hooke's law.

4.3. Hydraulic Capacitance Measurement. Hydraulic capacitance was measured using a custom-made machine (Figure 2). The controller adjusts the rotating speed of the motor so that the connected lifting plate moves vertically at a constant speed, which was set at 16.3 cm/min in all tests. The indicator was glued to the lifting plate so that the position on the ruler showed the maximal membrane deflection, which was determined by using a pixel analysis of the photographs captured by camera. A hemispherical press head was firmly clamped above the modular pump. Membranes of the same size but with distinct thicknesses (0.5 and 1 mm) were prepared for the modular pump. The modular pump and connecting tube were initially filled with

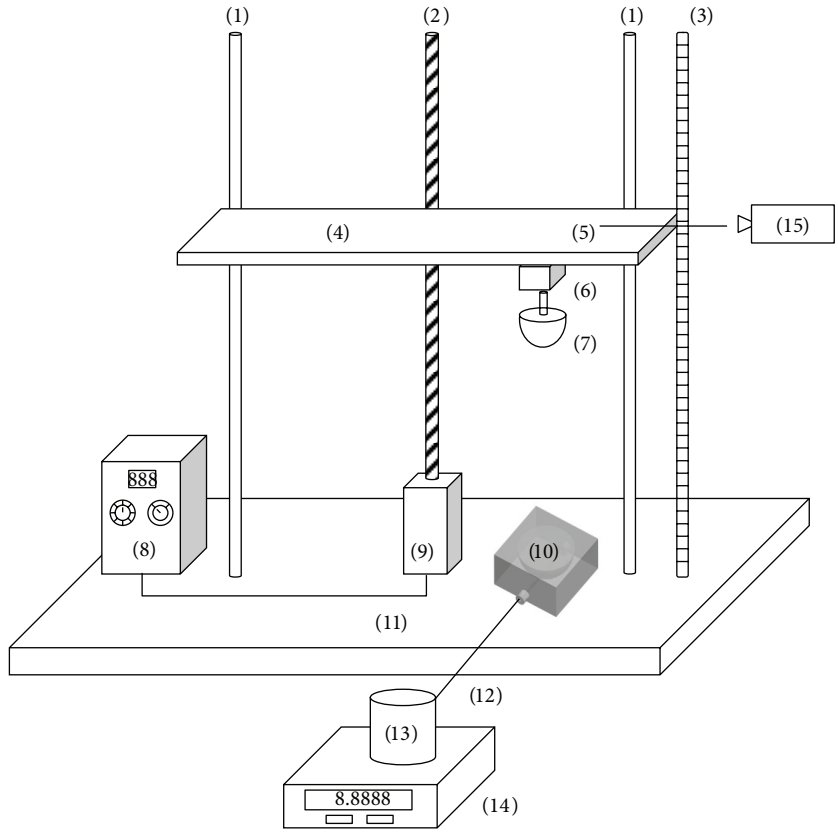

Not in scale

(1) Holding rod
(2) Screwed rod
(3) Ruler
(4) Lifting plate
(5) Indicator
(6) Clamp
(7) Hemispherical press head
(8) Controller
(9) Motor
(10) PDMS- made modular pump
(11) Base plate
(12) Connecting tube
(13) Paper cup
(14) Electric balance
(15) Camera

Figure 2: Scheme of custom-made apparatus for hydraulic capacitance measurement of modular membrane pump.

water. All bubbles were removed during the water injection procedure; thus, the membranes should remain flat when the pump is fully charged with water. After the hemispherical press head moved down and the modular pump membrane was pressed, water inside the pumping chamber discharged through the connecting tube to a paper cup on the electric balance. When the press descended to a certain depth, the indicator position on the ruler and the mass change on the electronic balance were recorded to determine the center deflection of the membrane and volume change of the modular pump. The modular pump was subsequently refilled to repeat the hydraulic capacitance measurement. The pressure was determined by measuring the center deflection, which was substituted into (7) or (8). After the volume change was measured, the hydraulic capacitance was determined using $\Delta V/\Delta p = (V_i - V_o)/(p_i - p_o)$, where V_i and p_i are the volume and pressure at any instant with applied pressure. The experimental error was calculated based on the pixel analysis error; this was determined using the misjudged pixels divided by the pixels of minimal scale on the ruler, multiplied by the measured center deflection. After calculation, the error ranged from 2.48% to 28.4%.

5. Results and Discussion

Figure 3 shows the relation between Young's modulus of the PDMS membrane and the inverse of the square root of the thickness. Each data point corresponds to the averaged value of eight samples. Though 10 samples for each thickness were measured, to reduce the uncertainty, eight samples were averaged instead of 10. The error bar is designated by $\pm 2\sigma_{sd}$, where σ_{sd} indicates the standard deviation. After calculation, the uncertainties for the elastic moduli were 6.86%, 7.57%, 5.63%, and 8.99% for PDMS membrane thicknesses of 0.3, 0.5, 0.7,

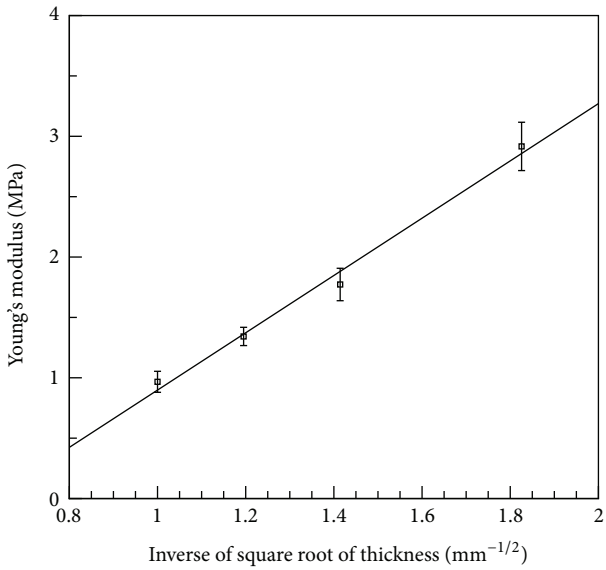

Figure 3: Young's modulus of the PDMS membrane versus the inverse of the square root of the thickness.

and 1 mm, respectively, indicating that Young's moduli of the PDMS membranes increased linearly as the thickness decreased. The experimental data for Young's moduli of the PDMS membrane were fitted using a linear fitting: $E = 75.03h^{-1/2} - 1.4744$, for $h = 0.3$–1 mm. This indicated that following the fabrication procedures discussed in Section 4.1 enabled Young's modulus of a PDMS membrane to be predicted using this linear trend line. Therefore, the elastic moduli of various PDMS membrane thicknesses for (12)–(15) can be determined.

To qualitatively describe the hydraulic capacitance without considering the influence of thickness and the elastic modulus of membrane, the dimensionless variables of the linear and nonlinear regions were proposed and defined as $\delta^* = \delta/R$, $C^*_{\text{linear}} = C_h/C_o$, and $C^*_{\text{nonlinear}} = C_h/C_R$, where C_h is the hydraulic capacitance, C_o is the original hydraulic capacitance (hydraulic capacitance when δ = zero), and C_R is the hydraulic capacitance of (13) when δ equals R. Substituting these dimensionless variables yields dimensionless hydraulic capacitance equations for the linear and nonlinear regions as follows:

$$C^*_{\text{linear}} = \left(\frac{\partial V_{\text{deflection}}/\partial p + \left(\partial V_{\text{deflection}}/\partial h\right)\left(\Delta h/\Delta p\right)}{C_o} \right)_{\text{linear}} = 1 + 4\delta^{*2}, \tag{16}$$

$$C^*_{\text{linear}} = \left(\frac{\partial V_{\text{deflection}}/\partial p}{C_o} \right)_{\text{linear}} = 1 + \delta^{*2}, \tag{17}$$

$$C^*_{\text{linear}} = \left(\frac{\Delta V_{\text{deflection}}/\Delta p}{C_o} \right)_{\text{linear}} = 1 + \frac{\delta^{*2}}{3}, \tag{18}$$

Table 1: Average errors among measured data and (16)–(21).

	Measured data when $h/R = 0.0649$	Measured data when $h/R = 0.1299$
Equations for linear region		
Equation (16)	10.87%	12.99%
Equation (17)	11.91%	15.5%
Equation (18)	12.15%	16.08%
Equations for nonlinear region		
Equation (19)	235.57%	299.35%
Equation (20)	205.75%	240.73%
Equation (21)	8.19%	25.66%

$$C^*_{\text{nonlinear}} = \left(\frac{\partial V_{\text{deflection}}/\partial p}{C_R} + \frac{\left(\partial V_{\text{deflection}}/\partial h\right)\left(\Delta h/\Delta p\right)}{C_R} \right)_{\text{nonlinear}} = \frac{1}{1+\delta^{*2}}\left(1 + \frac{1}{\delta^{*2}}\right), \tag{19}$$

$$C^*_{\text{nonlinear}} = \left(\frac{\partial V_{\text{deflection}}/\partial p}{C_R} \right)_{\text{linear}} = \left(1 + \frac{1}{\delta^{*2}}\right), \tag{20}$$

$$C^*_{\text{nonlinear}} = \left(\frac{\Delta V_{\text{deflection}}/\Delta p}{C_R} \right)_{\text{nonlinear}} = \left(1 + \frac{3}{\delta^{*2}}\right). \tag{21}$$

Figure 4 shows a comparison of the dimensionless experimental results and (16)–(18) regarding hydraulic capacitance in the linear region: (a) plotted as $h/R = 0.1299$; (b) plotted as $h/R = 0.0649$. The measured data were around 15% higher than the predicted values. The data were close to (16), exhibiting an error range of 7.26%–15.36%. Although the theoretical predictions tended to increase, the experimental results fluctuated. Figure 5 shows a comparison of the dimensionless experimental results and (19)–(21) regarding hydraulic capacitance in the nonlinear region: (a) plotted as $h/R = 0.1299$; (b) plotted as $h/R = 0.0649$. The data were close to (21), exhibiting an error range of 6.91%–44.77%. The results show that the hydraulic capacitance is not constant throughout the regions; this is inconsistent with the well-known characteristics of capacitors in electric circuits. In the linear region, the measured data fluctuated and were slightly higher than the theoretical predictions. However, the nonlinear region initially exhibited a drastic increase at the intersection of the linear and nonlinear regions that subsequently decayed. Table 1 lists the average deviations of the measured data and (16)–(21). The deviations of the measured data and (16)–(18) were small in the linear region. Although the equations used in quick estimations did not substantially differ in the linear region, compared with (19) and (20), (21) was closer to the measured data in the nonlinear region. The deviations of the measured data and (19) and (20) were huge in the nonlinear region; we believe that the errors mostly come from neglecting the elasticity term.

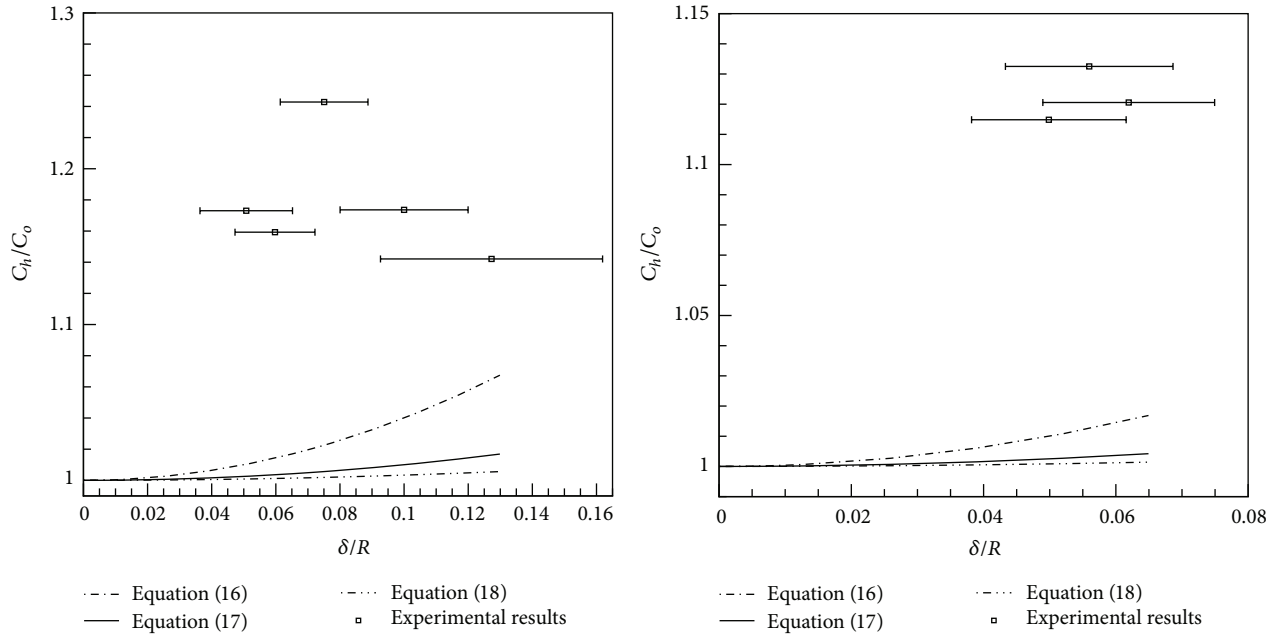

(a) $h/R = 0.1299$ (b) $h/R = 0.0649$

Figure 4: Comparison of the dimensionless experimental results and (16)–(18) regarding hydraulic capacitance in the linear region: (a) plotted as $h/R = 0.1299$; (b) plotted as $h/R = 0.0649$.

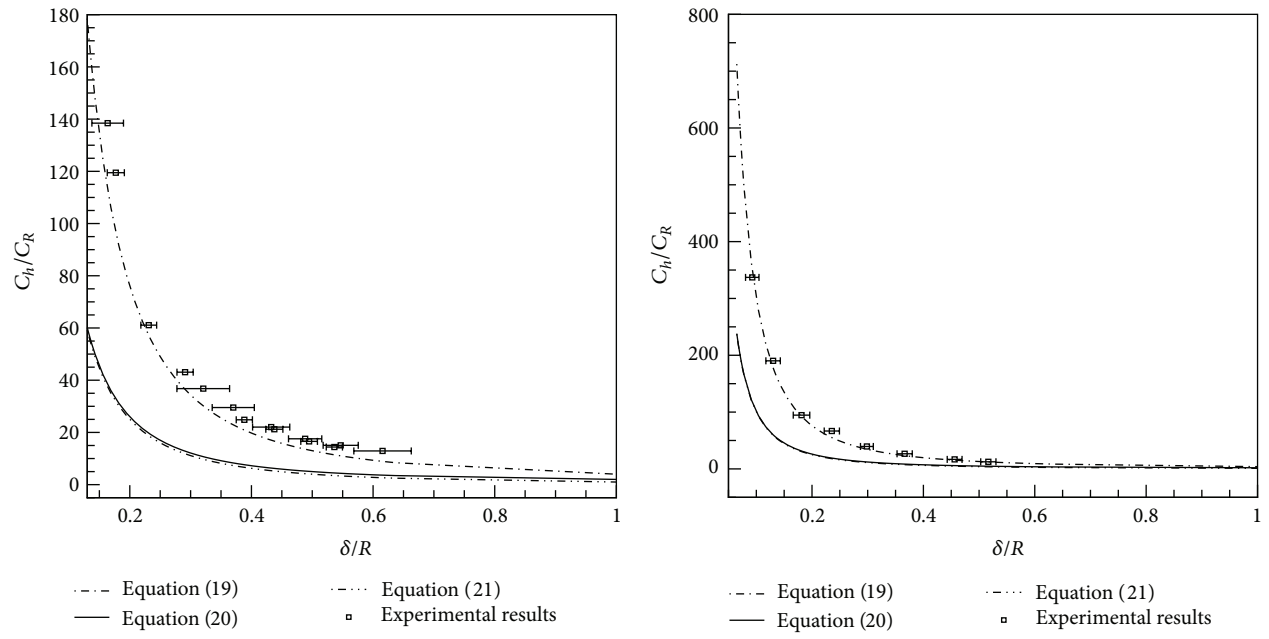

(a) $h/R = 0.1299$ (b) $h/R = 0.0649$

Figure 5: Comparison of the dimensionless experimental results and (19)–(21) regarding hydraulic capacitance in the nonlinear region: (a) plotted as $h/R = 0.1299$; (b) plotted as $h/R = 0.0649$.

6. Conclusion

In this study, a novel approach was proposed to measure the hydraulic capacitance of a microfluidic membrane pump. Two parameters were measured: the volume change of the membrane pump and the center deflection of the membrane when external force was applied. Instead of measuring pressure inside the pumping chamber, the center deflection of the membrane was measured and substituted into theoretical equations to determine the corresponding pressure. Various studies have proposed pressure-deflection relations for circular and boundary-bonded membranes [6,

12, 14–16]. Using those relations, this study further simplified and proposed four new theoretical relations ((12), (13), and (15)) to estimate the hydraulic capacitance of a microfluidic membrane pump. The measured hydraulic capacitance of the microfluidic membrane pump is determined based on the volume change of the membrane pump divided by the corresponding pressure.

This study also investigated the relationship between Young's modulus and membrane thickness. A linear correlation was proposed after fitting the experimental results as follows: $E = 75.03h^{-0.5} - 1.4744$, for $h = 0.3$–1 mm. Applying this relation of Young's modulus yields enhanced hydraulic capacitance estimations.

The dimensionless hydraulic capacitance measurement results show that the measured data fluctuated and were around 15% higher compared with the theoretical predictions in the linear region. Regarding the nonlinear region, the values drastically increased and subsequently decayed, similar to the trend exhibited by the theoretical predictions proposed in this study. The proposed dimensionless (18) and (21) are suggested to be used in qualitative estimations because they were the experimental limits of the proposed measurement approach.

Abbreviations

PDMS: Polydimethylsiloxane
EAT: Electrohydraulic analogy theory.

Conflict of Interests

The authors declare that there is no conflict of interests regarding the publication of this paper.

Acknowledgments

The authors thank Professors Chao-Sung Lin and Chun-Hway Hsueh from the Department of Materials Science and Engineering of National Taiwan University for providing the apparatus used in the study. Financial support was provided by the National Science Council, Taiwan (Grants NSC 102-2221-E002-133-MY3 and NSC 102-2221-E002-088-MY3), and Yen Tjing Ling Industrial Research Institute, National Taiwan University (Grant 102-S-A13).

References

[1] J. Xie, J. Shih, Q. Lin, B. Yang, and Y.-C. Tai, "Surface micromachined electrostatically actuated micro peristaltic pump," *Lab on a Chip—Miniaturisation for Chemistry and Biology*, vol. 4, no. 5, pp. 495–501, 2004.

[2] M. Koch, N. Harris, A. G. R. Evans, N. M. White, and A. Brunnschweiler, "A novel micromachined pump based on thick-film piezoelectric actuation," *Sensors and Actuators A: Physical*, vol. 70, no. 1-2, pp. 98–103, 1998.

[3] S. Böhm, W. Olthuis, and P. Bergveld, "Plastic micropump constructed with conventional techniques and materials," *Sensors and Actuators A: Physical*, vol. 77, no. 3, pp. 223–228, 1999.

[4] C. Yamahata, F. Lacharme, Y. Burri, and M. A. M. Gijs, "A ball valve micropump in glass fabricated by powder blasting," *Sensors and Actuators B: Chemical*, vol. 110, no. 1, pp. 1–7, 2005.

[5] D.-S. Liou, Y.-F. Hsieh, L.-S. Kuo, C.-T. Yang, and P.-H. Chen, "Modular component design for portable microfluidic devices," *Microfluidics and Nanofluidics*, vol. 10, no. 2, pp. 465–474, 2011.

[6] M. M. Gong, B. D. MacDonald, T. Vu Nguyen, and D. Sinton, "Hand-powered microfluidics: a membrane pump with a patient-to-chip syringe interface," *Biomicrofluidics*, vol. 6, no. 4, Article ID 044102, 2012.

[7] W. Li, T. Chen, Z. Chen et al., "Squeeze-chip: a finger-controlled microfluidic flow network device and its application to biochemical assays," *Lab on a Chip—Miniaturisation for Chemistry and Biology*, vol. 12, no. 9, pp. 1587–1590, 2012.

[8] A.-S. Yang, Y.-F. Hsieh, L.-S. Kuo, L.-Y. Tseng, S.-K. Liao, and P.-H. Chen, "A novel vortex mixer actuated by one-shot electricity-free pumps," *Chemical Engineering Journal*, vol. 228, pp. 882–888, 2013.

[9] R. E. Oosterbroek, T. S. J. Lammerink, J. W. Berenschot, G. J. M. Krijnen, M. C. Elwenspoek, and A. van den Berg, "Micromachined pressure/flow-sensor," *Sensors and Actuators A: Physical*, vol. 77, no. 3, pp. 167–177, 1999.

[10] S. Choi, M. G. Lee, and J.-K. Parka, "Microfluidic parallel circuit for measurement of hydraulic resistance," *Biomicrofluidics*, vol. 4, no. 3, Article ID 034110, 2010.

[11] A. Akers, M. Gassman, and R. Smith, *Hydraulic Power System Analysis*, CRC Press, New York, NY, USA, 2010.

[12] V. Tesař, *Pressure-Driven Microfluidics: Artech House Integrated Microsystems*, Artech House, Norwood, Mass, USA, 2007.

[13] V. Tesař and J. Kordík, "Effective hydraulic resistance of a nozzle in an electrodynamic actuator generating hybrid-synthetic jet—part I: data acquisition," *Sensors and Actuators A: Physical*, vol. 199, pp. 379–390, 2013.

[14] J. P. Landers, *Handbook of Capillary and Microchip Electrophoresis and Associated Microtechniques*, CRC Press, New York, NY, USA, 2007.

[15] M. Elwenspoek and R. Wiegerink, *Mechanical Microsensors*, Springer, New York, NY, USA, 2001.

[16] T.-R. Hsu, *MEMS & Microsystems: Design, Manufacture, and Nanoscale Engineering*, John Wiley & Sons, New York, NY, USA, 2008.

[17] M. Liu, J. Sun, Y. Sun, C. Bock, and Q. Chen, "Thickness-dependent mechanical properties of polydimethylsiloxane membranes," *Journal of Micromechanics and Microengineering*, vol. 19, no. 3, Article ID 035028, 2009.